

# VIDE: The Void IDentification and Examination Toolkit

P. M. Sutter<sup>a,b,c</sup>, Guilhem Lavaux<sup>a,b</sup>, Nico Hamaus<sup>a,b</sup>, Alice Pisani<sup>a,b</sup>, Benjamin D. Wandelt<sup>a,b,d,e</sup>, Mike Warren<sup>f</sup>, Francisco Villaescusa-Navarro<sup>g,h</sup>, Paul Zivick<sup>i</sup>, Qingqing Mao<sup>j</sup>, Benjamin B. Thompson<sup>k</sup>

<sup>a</sup>*Sorbonne Universités, UPMC Univ Paris 06, UMR7095, Institut d'Astrophysique de Paris, F-75014, Paris, France*

<sup>b</sup>*CNRS, UMR7095, Institut d'Astrophysique de Paris, F-75014, Paris, France*

<sup>c</sup>*Center for Cosmology and AstroParticle Physics, Ohio State University, Columbus, OH 43210, USA*

<sup>d</sup>*Department of Physics, University of Illinois at Urbana-Champaign, Urbana, IL 61801, USA*

<sup>e</sup>*Department of Astronomy, University of Illinois at Urbana-Champaign, Urbana, IL 61801, USA*

<sup>f</sup>*Theoretical Division, Los Alamos National Laboratory, Los Alamos, NM 87545, USA*

<sup>g</sup>*INAF - Osservatorio Astronomico di Trieste, Via Tiepolo 11, I-34143, Trieste, Italy*

<sup>h</sup>*INFN sez. Trieste, Via Valerio 2, I-34127, Trieste, Italy*

<sup>i</sup>*Department of Astronomy, Ohio State University, Columbus, OH 43210, USA*

<sup>j</sup>*Department of Physics and Astronomy, Vanderbilt University, Nashville, TN 37235, USA*

<sup>k</sup>*Jeremiah Horrocks Institute, University of Central Lancashire, Preston, PR1 2HE, United Kingdom*

arXiv:1406.1191v2 [astro-ph.CO] 17 Oct 2014

---

## Abstract

We present VIDE, the Void IDentification and Examination toolkit, an open-source Python/C++ code for finding cosmic voids in galaxy redshift surveys and  $N$ -body simulations, characterizing their properties, and providing a platform for more detailed analysis. At its core, VIDE uses a substantially enhanced version of ZOBOV (Neyinck 2008) to calculate a Voronoi tessellation for estimating the density field and a performing a watershed transform to construct voids. Additionally, VIDE provides significant functionality for both pre- and post-processing: for example, VIDE can work with volume- or magnitude-limited galaxy samples with arbitrary survey geometries, or dark matter particles or halo catalogs in a variety of common formats. It can also randomly subsample inputs and includes a Halo Occupation Distribution model for constructing mock galaxy populations. VIDE uses the watershed levels to place voids in a hierarchical tree, outputs a summary of void properties in plain ASCII, and provides a Python API to perform many analysis tasks, such as loading and manipulating void catalogs and particle members, filtering, plotting, computing clustering statistics, stacking, comparing catalogs, and fitting density profiles. While centered around ZOBOV, the toolkit is designed to be as modular as possible and accommodate other void finders. VIDE has been in development for several years and has already been used to produce a wealth of results, which we summarize in this work to highlight the capabilities of the toolkit. VIDE is publicly available at [http://bitbucket.org/cosmicvoids/vid\\_public](http://bitbucket.org/cosmicvoids/vid_public) and <http://www.cosmicvoids.net>.

*Keywords:* cosmology: large-scale structure of universe, methods: data analysis

---

## 1. Introduction

Cosmic voids are emerging as a novel probe of both cosmology and astrophysics, as well as fascinating objects of study themselves. These large empty regions in the cosmic web, first discovered over thirty years ago (Gregory and Thompson 1978; Jöeveer et al. 1978; Kirshner et al. 1981), are now known to fill up nearly the entire volume of the Universe (Hoyle and Vogeley 2004; Pan et al. 2012; Sutter et al. 2012b). These voids exhibit some intriguing properties. For example, while apparently just simple vacant spaces, they actually contain a complex, multi-level hierarchical dark matter substructure (van de Weygaert and van Kampen 1993; Gottlober et al. 2003; Aragon-Calvo and Szalay 2013). Indeed, the interiors of voids appear as miniature cosmic webs, albeit at a different mean density (Goldberg and Vogeley 2004). However, these void

substructures obey simple scaling relations that enable direct translations of void properties between different tracer types (e.g., galaxies and dark matter) (Benson et al. 2003; Ricciardelli et al. 2014; Sutter et al. 2013a). Their internal growth is relatively simple: voids do not experience major merger events over their long lifetimes (Sutter et al. 2014b) and their interiors are largely unaffected by larger-scale environments (Dubinski et al. 1993; Fillmore and Goldreich 1984; van de Weygaert et al. 2010b).

As underdense regions, voids are the first objects in the large-scale structure to be dominated by dark energy. This fact coupled with their simple dynamics makes them a unique and potentially potent probe of cosmological parameters, either through their intrinsic properties (e.g., Biswas et al. 2010; Bos et al. 2012), exploitation of their statistical isotropy via the Alcock-Paczyński test (Lavaux and Wandelt 2012; Sutter et al. 2012a, 2014d), or cross-correlation with the cosmic microwave background (Thompson and Vishniac 1987; Granett et al. 2008; Ilić et al. 2013;

---

*Email address:* [sutter@iap.fr](mailto:sutter@iap.fr) (P. M. Sutter)

Planck Collaboration 2013; Cai et al. 2014). Additionally, fifth forces and modified gravity are unscreened in void environments, making them singular probes of exotic physics (e.g., Li et al. 2012; Clampitt et al. 2013; Spolyar et al. 2013; Carlesi et al. 2014).

Voids offer a unique laboratory for studying the relationship between galaxies and dark matter unaffected by complicated baryonic physics. As noted above, there appears to be a self-similar relationship between voids in dark matter distributions and voids in galaxies (Sutter et al. 2013a) via a universal density profile (Hamaus et al. 2014a; hereafter HSW). Void-galaxy cross-correlation analyses also reveal a striking feature: the large-scale clustering power of compensated voids is identically zero, which may give rise to a static cosmological ruler (Hamaus et al. 2014b). Observationally, measurements of the anti-lensing shear signal of background galaxies have revealed the internal dark matter substructure in voids (Melchior et al. 2014; Clampitt and Jain 2014), and Ly-alpha absorption measurements have illuminated dark matter properties in void outskirts (Tejos et al. 2012). Finally, studying the formation of void galaxies reveals the secular evolution of dark matter halos (Rieder et al. 2013) and their mass function (Neyrinck et al. 2014).

Voids present a useful region for investigating astrophysical phenomena, as well. For example, the detection of magnetic fields within voids constrains the physics of the primordial Universe (Taylor et al. 2011; Beck et al. 2013). Contrasting galaxies in low- and high-density environments probes the relationship between dark matter halo mass and galaxy evolution (van de Weygaert and Platen 2011; Kreckel et al. 2011; Ceccarelli et al. 2012; Hoyle et al. 2012).

Given the burgeoning interest in voids, there remains surprisingly little publicly-accessible void information. There are a few public catalogs of voids identified in galaxy redshift surveys, primarily the SDSS (e.g., Pan et al. 2012; Sutter et al. 2012b; Nadathur and Hotchkiss 2014; Sutter et al. 2013c, 2014d), and there are fewer still catalogs of voids found in simulations and mock galaxy populations (Sutter et al. 2013a). And while there are many published methods for finding voids based on a variety of techniques, such as spherical underdensities (Hoyle and Vogeley 2004; Padilla et al. 2005), watersheds (Platen et al. 2007; Neyrinck 2008), and phase-space dynamics (Lavaux and Wandelt 2010; van de Weygaert et al. 2010a; Sousbie 2011; Cautun et al. 2013; Neyrinck et al. 2013), most codes remain private. In order to accommodate the expanding application of voids and to engender the development of communities and collaborations, it is essential to provide easy-to-use, flexible, and strongly supported void-finding codes.

In this paper we present `VIDE`<sup>1</sup>, for Void IDentification and Examination, a toolkit based on the publicly-available

watershed code `ZOBOV` (Neyrinck 2008) for finding voids but considerably enhanced and extended to handle a variety of simulations and observations. `VIDE` also provides an extensive interface for analyzing void catalogs. In Section 2 we outline the input data options for void finding, followed by Section 3 where we describe our void finding technique and our extensions and modifications to `ZOBOV`. Section 4 details our Python-based analysis toolkit functionality, and Section 5 is a quick-start user’s guide. We summarize and provide an outlook for future uses and upgrades to `VIDE` in Section 6.

## 2. Input Data Options

### 2.1. Simulations

To identify voids in  $N$ -body dark matter populations, `VIDE` is able to read `Gadget` (Springel 2005), `FLASH` (Dubey et al. 2008), and `RAMSES` (Teyssier 2002) simulation outputs, files in the Self-Describing Format (Warren 2013), and generic ASCII files listing positions and velocities. Void finding can be done on the dark matter particles themselves, or in randomly subsampled subsets with user-defined mean densities. Subsampling can be done either in a post-processing step or *in situ* during void finding.

`VIDE` can also find voids in halo populations. The user must provide an ASCII file and specify the columns containing the halo mass, position, and other properties. The user can use all identified halos or specify a minimum mass threshold for inclusion in the void finding process.

The user may construct a mock galaxy population from a halo catalog using a Halo Occupation Distribution (HOD) formalism (Berlind and Weinberg 2002). HOD modeling assigns central and satellite galaxies to a dark matter halo of mass  $M$  according to a parametrized distribution. `VIDE` implements the five-parameter model of Zheng et al. (2007), where the mean number of central galaxies is given by

$$\langle N_{\text{cen}}(M) \rangle = \frac{1}{2} \left[ 1 + \text{erf} \left( \frac{\log M - \log M_{\text{min}}}{\sigma_{\log M}} \right) \right] \quad (1)$$

and the mean number of satellites is given by

$$\langle N_{\text{sat}}(M) \rangle = \langle N_{\text{cen}}(M) \rangle \left( \frac{M - M_0}{M'_1} \right)^\alpha, \quad (2)$$

where  $M_{\text{min}}$ ,  $\sigma_{\log M}$ ,  $M_0$ ,  $M'_1$ , and  $\alpha$  are free parameters that must be fitted to a given survey. The probability distribution of central galaxies is a nearest-integer distribution (i.e., all halos above a given mass threshold host a central galaxy), and satellites follow Poisson statistics. These satellites are placed around the central galaxy with random positions assuming a probability given by the NFW (Navarro et al. 1996) profile for a halo of the given mass. The user can also specify an overall mean density in case the HOD model was generated from a simulation with different cosmological parameters than the one used

<sup>1</sup>The French word for “empty”.

for void finding, which causes a mismatch in the target galaxy density. While not a full fix (which would require a new HOD fit), this at least alleviates some of the mismatch.

We have included — but not fully integrated into the pipeline — a separate code for fitting HOD parameters to a given simulation. The implemented model has three parameters, and given two of those the third is fixed by demanding that the abundance of galaxies of a given population reproduces the observed value. We then explore the 2-dimensional space of the other two parameters trying to minimize the  $\chi^2$  that results from comparing the two-point correlation function of the simulated galaxies with the observed data.

In all cases (particles, halos, or mock galaxies), void finding can be done on the real-space particle positions or after being placed on a lightcone (i.e., redshift space) assuming given cosmological parameters, where the  $z$ -axis of the simulation is taken to be the line of sight. Voids can also be found after particle positions have been perturbed using their peculiar velocities. The user may define independent slices and sub-boxes of the full simulation volume, and VIDE will handle all periodic effects and boundary cleaning (see Section 3) automatically.

## 2.2. Observations

In addition to providing an ASCII file listing galaxy right ascension, declination, and redshift, the user must provide a pixelization of the survey mask using HEALPIX (Gorski et al. 2005)<sup>2</sup>. The HEALPIX description of the sphere provides equal-area pixels, and the HEALPIX implementation itself provides built-in tools to easily determine which pixels lie on the boundary between the survey area and any masked region. This is essential for VIDE to constrain voids to the survey volume (see Section 3). Figure 1 shows a pixelization of the SDSS DR9 mask and the location of the boundary pixels. To accurately capture the shape of the mask we require a resolution of at least  $n_{\text{side}} = 512$ .

VIDE also provides a utility for constructing a rudimentary mask from the galaxy positions themselves.

The default VIDE behavior is to assume that the galaxy population is volume-limited (i.e., uniform galaxy density as a function of redshift). However, the user may provide a selection function and identify voids in a full magnitude-limited survey. As mentioned in Neyrinck (2008), in this case the Voronoi densities will be weighted prior to void finding such that  $\rho' = \rho/w(z)$ , where  $w(z)$  is the relative number density as a function of redshift (note that this functionality can also be used for arbitrary re-weighting, if desired). This re-weighting is only used in the watershed phase for purposes of constructing voids, and does not enter into later volume or density calculations. If re-weighting is chosen then the selection function will be used to calculate a global mean density.

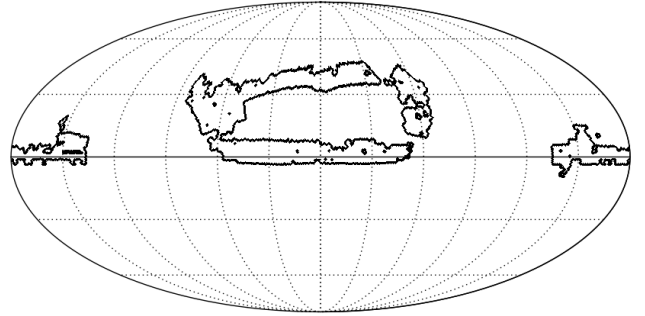


Figure 1: Example HEALPIX map in a Mollweide projection of identified boundary zones (black) around and within the SDSS DR9 survey area. Maps like this are used to prevent voids from being identified outside a survey volume. *Reproduced from Sutter et al. (2013c).*

## 3. Void Finding

The core of our void finding algorithm is ZOBOV (Neyrinck 2008), which creates a Voronoi tessellation of the tracer particle population and uses the watershed transform to group Voronoi cells into zones and subsequently voids (Platen et al. 2007). The Voronoi tessellation provides a density field estimator based on the underlying particle positions. By implicitly performing a Delaunay triangulation (the dual of the Voronoi tessellation), ZOBOV assumes constant density across the volume of each Voronoi cell, which effectively sets a local smoothing scale for the continuous field necessary to perform the watershed transform. There is no additional smoothing. For magnitude-limited surveys, where the mean galaxy density varies as a function of redshift, we weight the Voronoi cell volumes by the local value of the radial selection function.

To construct voids the algorithm first groups nearby Voronoi cells into zones, which are local catchment basins. Next, the watershed transform merges adjacent zones into voids by finding minimum-density barriers between them and joining zones together to form larger agglomerations. We impose a density-based threshold within ZOBOV where adjacent zones are only added to a void if the density of the wall between them is less than 0.2 times the mean particle density  $\bar{n}$ . For volume-limited surveys we calculate the mean particle density by dividing the survey volume (from the HEALPIX mask and redshift extents) by the total number of galaxies. For magnitude-limited surveys the mean particle density is estimated from the selection function. This density criterion prevents voids from expanding deeply into overdense structures and limits the depth of the void hierarchy (Neyrinck 2008).

However, this process does not place a restriction on the density of the initial zone, and thus in principle a void can have any minimum density. By default VIDE reports every identified basin as a void, but in the section below we describe some provided facilities for filtering the catalog based on various criteria, depending on the specific user application.

<sup>2</sup><http://healpix.jpl.nasa.gov>

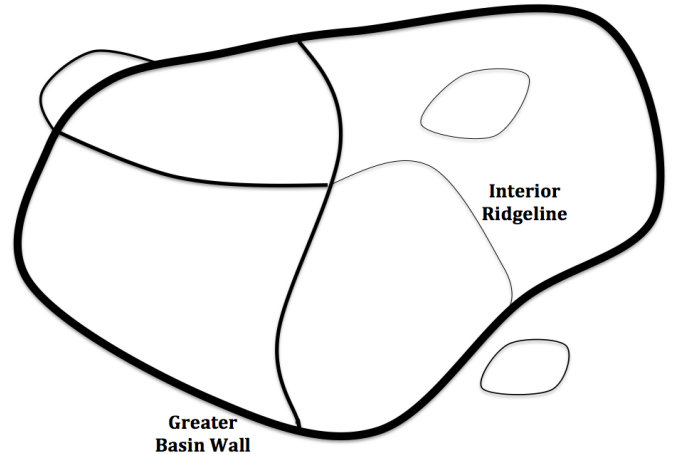
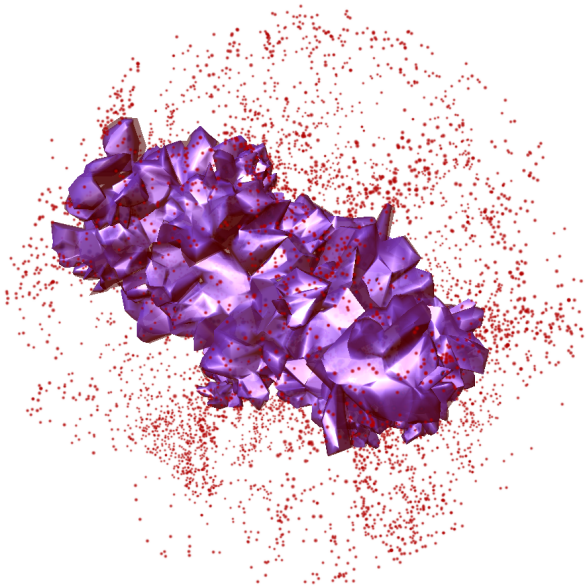


Figure 2: An example of a watershed void in VIDE. The Voronoi cells that define the void are in purple with galaxies in red. We show a void with effective radius  $20 h^{-1}\text{Mpc}$  within a  $50 h^{-1}\text{Mpc}$  spherical region. Galaxy point sizes are proportional to their distance from the point of view. Galaxies interior to the void are shaded dark red. *Reproduced from Sutter et al. (2012b).*

In this picture, a void is simply a depression in the density field: voids are aspherical aggregations of Voronoi cells that share a common low-density basin and are bounded by a common set of higher-density walls, as demonstrated by Figure 2, which shows a typical  $20 h^{-1}\text{Mpc}$  void identified in the SDSS DR7 galaxy survey (Sutter et al. 2012b). This also means that voids may have any *mean* density, since the watershed includes in the void definition all wall particles all the way up to the very highest-density separating ridgeline.

We may construct a nested hierarchy of voids (Lavaux and Wandelt 2012; Bos et al. 2012) using the topologically-identified watershed basins and ridgelines. We begin by identifying the initial zones as the deepest voids, and as we progressively merge voids across ridgelines we establish super-voids. There is no unique definition of a void hierarchy, and we take the semantics of Lavaux and Wandelt (2012): a parent void contains all the zones of a sub-void plus at least one more. All voids have only one parent but potentially many children, and the children of a parent occupy distinct subvolumes separated by low-lying ridgelines. There are also childless “field” voids. Figure 3 shows a cartoon of this void hierarchy construction. Without the application of the  $0.2\bar{n}$  density cut discussed above, ZOBOV would identify a single super-void spanning the entire volume, and thus there would be a single hierarchical tree. However, with the cut applied there are multiple top-level voids.

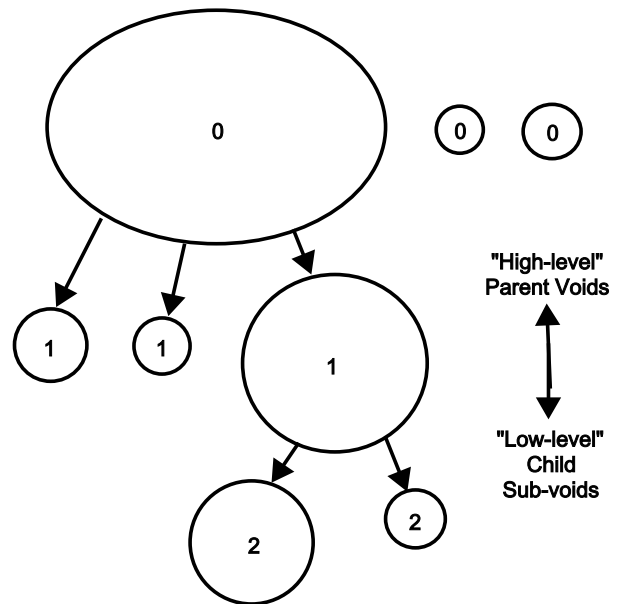


Figure 3: A cartoon of the assembly of the void hierarchy. The top panel shows ridgelines with line thickness proportional to density. The bottom panel shows the tree derived from such a collection of voids, with the tree level of each void indicated. *Reproduced from Sutter et al. (2014b).*

For historical reasons (Sutter et al. 2012a,b), the default catalog removes voids with high central densities ( $\rho(R < 0.25R_{\text{eff}}) > 0.2\bar{\rho}$ ) and any children voids, but the user can trivially access all voids.

We have made several modifications and improvements to the original ZOBOV algorithm, which itself is an inversion of the halo-finding algorithm VOBOZ (Neyrinck et al. 2005). First, we have made many speed and performance enhancements, as well as re-written large portions in a templated C++ framework for more modularity and flexibility. This strengthens ZOBOV with respect to numerical precision. Floating-point precision can occasionally lead to disjoint Voronoi graphs, especially in high-density regions: one particle may be linked to another while its partner does not link back to it. We therefore enforce bijectivity in the Voronoi graph (so that the tessellation is self-consistent) by ensuring that all links are bidirectional.

We apply ZOBOV to very large simulations. To run the analysis on such simulations while keeping memory consumption within reasonable bounds, it is necessary to split the volume on which the Delaunay tessellation is done into several subvolumes. Additionally many large simulations store the particle positions in single precision mode. The original ZOBOV re-shifted each subvolume such that their geometrical center was always at the coordinate  $(0, 0, 0)$ . However that involves computing differences with single precision floats, increasing the numerical noise. We found practically that shifting the subvolume to place a corner at  $(0, 0, 0)$  incurs slightly fewer problems. However, this is insufficient to completely mitigate the issue that when subvolumes are merged the volumes of the tetrahedra are not exactly the same on both sides of the subvolume boundary. So we again enforce the connectivity of the mesh, but lose the Delaunay properties at each subvolume boundary. While this is not exact, it still constructs a fully connected mesh and allows the computation of the watershed transform.

Finally, we have improved the performance of the watershed transform in ZOBOV using a priority queue algorithm to sort out the zones that need to be processed according to their core density and spilling density (the saddle point with the minimum density). The priority queue algorithm has a  $\mathcal{O}(1)$  time complexity for getting the next element and replaces the  $\mathcal{O}(N)$  full search algorithm from the original ZOBOV. The cost of insertion is at most the number of zones that were not processed but in practice this is negligible. With these improvements we have identified voids in simulations with up to  $1024^3$  particles in  $\sim 10$  hours using 16 cores.

By default VIDE also use the latest version of the `qhull` library<sup>3</sup> (Barber et al. 1996), where we take advantage of provided functions for constructing Voronoi graphs that are more stable in high-density regions.

Since ZOBOV was originally developed in the context of simulations with periodic boundary conditions, care must

be taken in observations and simulation sub-volumes. To prevent the growth of voids outside survey boundaries, we place a large number of mock particles along any identified edge (Figure 1) and along the redshift caps. The user inputs the density of mock particles, and VIDE places them randomly within the projected volume of the `healpix` pixels. To prevent spillover and misidentification of edge zones, studies indicate that the density of these mock particles should be at least the density of the sample studied, and preferably as high as computationally tolerable (Sutter et al. 2012b; Nadathur and Hotchkiss 2014; Sutter et al. 2013b). We assign essentially infinite density to these mock particles, preventing the watershed procedure from merging zones external to the survey. Since their local volumes are arbitrary, we prevent these mock particles from participating in any void by disconnecting their adjacency links in the Voronoi graph.

This process leaves a population of voids near — but not directly adjacent to — the survey edge, which can induce a subtle bias in the alignment distribution, affecting cosmological probes such as the Alcock-Paczyński test (Sutter et al. 2012a). Also, while these *edge* voids are indeed underdensities, making them useful for certain applications, their true extent and shape is unknown. VIDE thus provides two void catalogs: *all*, which includes every identified void, and *central*, where voids are guaranteed to sit well away from any survey boundaries or internal holes: the maximum distance from the void center to any member particle is less than the distance to the nearest boundary. Voids near any redshift caps (defined using the same criterion) are removed from all catalogs.

For subvolumes taken from a larger simulation box (see the discussion above for input data options), the edges of the subvolume are assumed to be periodic for purposes of the watershed, regardless of whether that edge is actually periodic or not. However, any void near a non-periodic edge is removed from all catalogs using the distance criterion described in the preceding paragraph, since these voids will have ill-defined extents. For all simulation-based catalogs there is no difference between the *all* and *central* catalogs.

We use the mean particle spacing to set a lower size limit for voids because of the effects of shot noise. VIDE does not include any void with effective radius smaller than  $\bar{n}^{-1/3}$ , where  $\bar{n}$  is the mean number density of the sample. We define the effective radius as

$$R_{\text{eff}} \equiv \left( \frac{3}{4\pi} V \right)^{1/3}, \quad (3)$$

where  $V$  is the total volume of all the Voronoi cells that make up the void.

Figure 4 shows an example void population with VIDE, taken from the analysis of Hamaus et al. (2014b). In this figure we show a slice from an  $N$ -body simulation, a set of mock galaxies painted onto the simulation using the HOD formalism discussed above, and the distribution of voids identified in the mock galaxies.

<sup>3</sup><http://www.qhull.org>

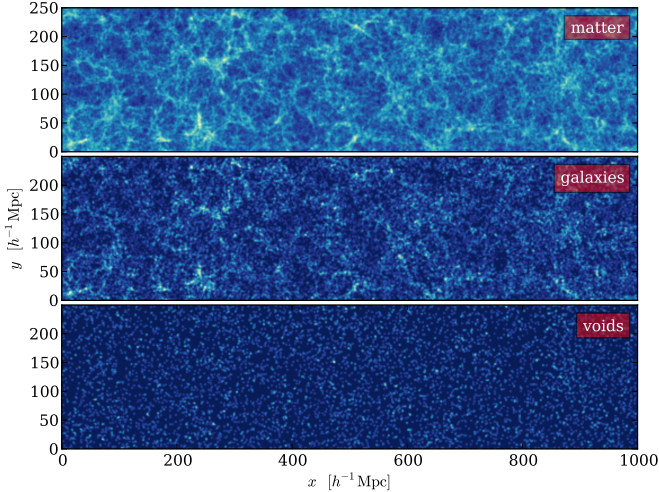


Figure 4: Projected density fields of dark matter (top), mock galaxies (middle) and voids (bottom) in a  $250h^{-1}\text{Mpc}$  slice of a simulation box. *Reproduced from Hamaus et al. (2014b)*.

VIDE provides some basic derived void information. The most important quantity is the *macrocenter*, or volume-weighted center of all the Voronoi cells in the void:

$$\mathbf{X}_v = \frac{1}{\sum_i V_i} \sum_i \mathbf{x}_i V_i, \quad (4)$$

where  $\mathbf{x}_i$  and  $V_i$  are the positions and Voronoi volumes of each tracer particle  $i$ , respectively. VIDE also computes void shapes by taking void member particles and constructing the inertia tensor:

$$\begin{aligned} M_{xx} &= \sum_{i=1}^{N_p} (y_i^2 + z_i^2) \\ M_{xy} &= -\sum_{i=1}^{N_p} x_i y_i \end{aligned} \quad (5)$$

where  $N_p$  is the number of particles in the void, and  $x_i$ ,  $y_i$ , and  $z_i$  are coordinates of the particle  $i$  relative to the void macrocenter. The other components of the tensor are obtained by cyclic permutations. This definition of the inertia tensor is designed to give greater weight to the particles near the void edge, which is useful for applications such as the Alcock-Paczyński test. Other definitions, such as volume-weighted tensors, can be implemented trivially with the toolkit functionality discussed below. We use the inertia tensor to compute eigenvalues and eigenvectors and form the ellipticity:

$$\epsilon = 1 - \left( \frac{J_1}{J_3} \right)^{1/4}, \quad (6)$$

where  $J_1$  and  $J_3$  are the smallest and largest eigenvalues of the inertia tensor, respectively.

## 4. Post-Processing & Analysis

VIDE provides a Python-based application programming interface (API) for loading and manipulating the void catalog and performing analysis and plotting. The utilities described below present simulation and observation void catalogs on an equal footing: density and volume normalizations, the presence of boundary particles, and other differences are handled internally by VIDE such that the user does not need to implement special cases, and simulations and observations may be directly compared to each other.

All the following analysis routines are compatible with releases of the Public Cosmic Void Catalog after version *2013.10.25*. Complete documentation is available at <http://bitbucket.org/cosmicvoids/vid-public/wiki/>.

### 4.1. Catalog Access

After loading a void catalog, the user has immediate access to all void properties (ID, macrocenter, radius, density contrast, RA, Dec, hierarchy level, ellipticity, etc.) as well as the positions ( $x, y, z$ , RA, Dec, redshift), velocities (if known), and local Voronoi volumes of all void member particles. By default these quantities are presented to the user as members of an object, but we provide a utility for selectively converting these quantities to NumPy arrays for more efficient processing. The user additionally has access to all particle or galaxy sample information, such as redshift extents, the mask, simulation extents and cosmological parameters, and other information. Upon request the user can also load all particles in the simulation or observation.

Since by default VIDE returns every void above the minimum size threshold set by the mean interparticle spacing of the sample, we provide some simple facilities for performing the most common catalog filtering. For example, the user may select voids based on size, position in the hierarchy, central density, minimum density, and density contrast.

### 4.2. Plotting

VIDE includes several built-in plotting routines. First, users may plot cumulative number functions of multiple catalogs on a logarithmic scale. Volume normalizations are handled automatically, and  $1\sigma$  Poisson uncertainties are shown as shaded regions, as demonstrated in Figure 5. Secondly, users may plot a slice from a single void and its surrounding environment. In these plots we bin the background particles onto a two-dimensional grid and plot the density on a logarithmic scale. We draw the void member galaxies as small semi-transparent disks with radii equal to the effective radii of their corresponding Voronoi cells. Figure 6 highlights these kinds of plots. The user may also plot an ellipticity distribution for any sample of voids. All plots are saved in png, pdf, and eps formats.

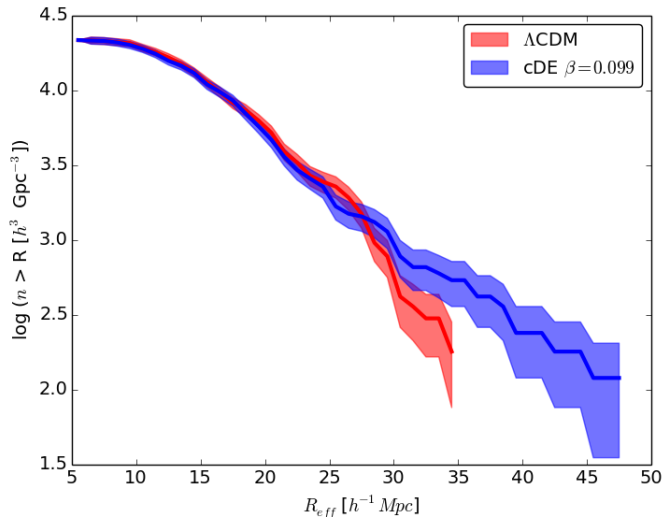


Figure 5: Example cumulative void number functions from simulations. Shown are abundances for  $\Lambda$ CDM (red) and a coupled dark matter-dark energy model (blue). The solid lines are the measured number functions and the shaded regions are the  $1\sigma$  Poisson uncertainties. *Reproduced from Sutter et al. (2014a).*

#### 4.3. Catalog Comparison

The user can directly compare two void catalogs by using a built-in function for computing the overlap. This function attempts to find a one-to-one match between voids in one catalog and another and reports the relative properties (size, ellipticity, etc.) between them. It also records which voids cannot find a reliable match and how many potential matches a void may have.

The potential matches are found by considering all voids in the matched void catalog whose centers lie within the watershed volume of the original void. Then for each potential matched void the user can choose to use either the unique particle IDs or the amount of volume overlap to find matches. We take the potential matched void with the greatest amount of overlap (volume or number of particles) as the best match.

In the case of volume overlap, to simplify the measurement we place each particle at the center of a sphere whose volume is the same as its Voronoi cell. We approximate the Voronoi volumes as spheres to provide a stricter definition of overlap, since the Voronoi volume can be highly elongated and lead to unwanted matching. We measure the distance between particles and assume they overlap if their distances meet the criterion

$$d \leq \alpha(R_1 + R_2), \quad (7)$$

where  $d$  is the distance and  $R_1$  and  $R_2$  are the radii of the spheres assigned to particles 1 and 2, respectively. The user may select the value  $\alpha$ , but we found the factor of  $\alpha = 0.25$  to strike the best balance between conservatively estimating overlap while still accounting for our spherical estimate of the Voronoi volume of each particle. If the particles meet the distance criterion, the volume is added

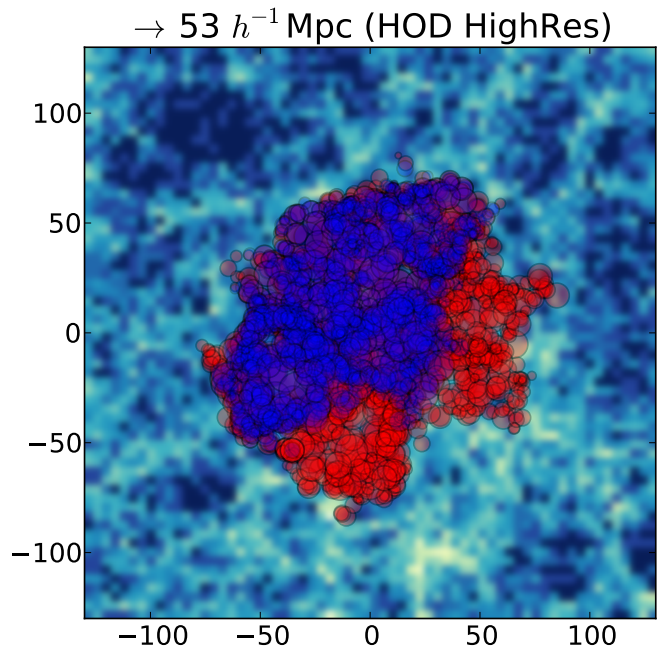


Figure 6: Example of matching and void plotting. Here a void identified in real space (blue circles) has been matched to a void identified in redshift space (red circles) in an HOD mock galaxy population. The background particles are binned and the corresponding density is shown on a logarithmic scale from 0.0 (white) to 1.5 (black). The void member galaxies are shown as small semi-transparent disks with radii equal to the effective radii of their corresponding Voronoi cells. In this case the width of the slice is  $50 h^{-1}$  Mpc. *Reproduced from Pisani et al. (2014).*

to the total amount of overlap; the void with the most amount of overlap is considered the best match.

A more detailed discussion of the matching process can be found in Sutter et al. (2014c). Figure 6 shows how a void identified in a real-space HOD mock galaxy population has been matched to a void identified in a corresponding redshift-space population.

#### 4.4. Clustering Statistics

VIDE allows the user to compute simple two-point clustering statistics, i.e. power spectra and correlation functions. To perform this, VIDE reads in particle positions and uses a cloud-in-cell mesh interpolation scheme (Hockney, R. W. & Eastwood, J. W. 1988) to construct a three-dimensional density field of fluctuations

$$\delta(\mathbf{r}) = \frac{n(\mathbf{r})}{\bar{n}} - 1, \quad (8)$$

where  $n(\mathbf{r})$  is the spatially varying number density of tracers with a mean of  $\bar{n}$ .

Then, Fourier modes of the density fluctuation with mesh wave vector  $\mathbf{k}$  are computed using a standard DFT algorithm (computed using an FFT),

$$\delta(\mathbf{k}) = \frac{1}{N_c} \sum_{\mathbf{r}} \delta(\mathbf{r}) \exp(-i\mathbf{k} \cdot \mathbf{r}), \quad (9)$$

and the angle-averaged power spectrum is estimated as

$$P(k) = \frac{V}{N_k} \sum_{\Delta k} \frac{|\delta(\mathbf{k})|^2}{W_{\text{cic}}^2(\mathbf{k})}. \quad (10)$$

Here  $V$  denotes the simulation volume,  $N_c$  the number of grid cells in the mesh,  $N_k$  the number of Fourier modes in a  $k$ -shell of thickness  $\Delta k$ , and

$$W_{\text{cic}}(\mathbf{k}) = \prod_{i=x,y,z} \frac{\sin^2(k_i)}{k_i^2} \quad (11)$$

is the cloud-in-cell window function to correct for artificial suppression of power originating from the mesh assignment scheme. An inverse Fourier transform of the power spectrum yields the correlation function,

$$\xi(r) = \frac{1}{V} \sum_{\mathbf{k}} P(\mathbf{k}) \exp(i\mathbf{k} \cdot \mathbf{r}). \quad (12)$$

As this procedure can be applied to any particle type, VIDE returns power spectra and correlation functions for both void centers and the tracer particles used to identify voids (e.g., dark matter particles or mock galaxies). In addition, it provides the cross-power spectrum and cross-correlation function between the void centers and the tracer particles. This routine creates plots for projected density fields (Figure 4) and power spectra and correlation functions (Figure 7).

#### 4.5. Stacking & Profiles

The user may construct three-dimensional stacks of voids, where void macrocenters are aligned and particle positions are shifted to be expressed as relative to the stack center. The stacked void may optionally contain only void member particles or all particles within a certain radius. Note that this stacking routine does not re-align observed voids to share a common line of sight. With this stacked profile VIDE contains routines for building a spherically averaged radial density profile and fitting the universal HSW void profile to it. All proper normalizations are handled internally. Figure 8 shows an example of VIDE-produced density profiles and best-fit HSW profile curves. These profiles are taken at fixed void size but from many different samples, such as high-density dark matter and mock galaxy populations.

VIDE also provides routines for reporting theoretical best-fit HSW profiles discovered in a variety of populations and void sizes, taken from Hamaus et al. (2014a) and Sutter et al. (2013a). The user can select the sample density, tracer type, and void size closest to their population of interest. These profiles are useful for many applications, such as ISW predictions and comparing theory to data (e.g., Pisani et al. 2013).

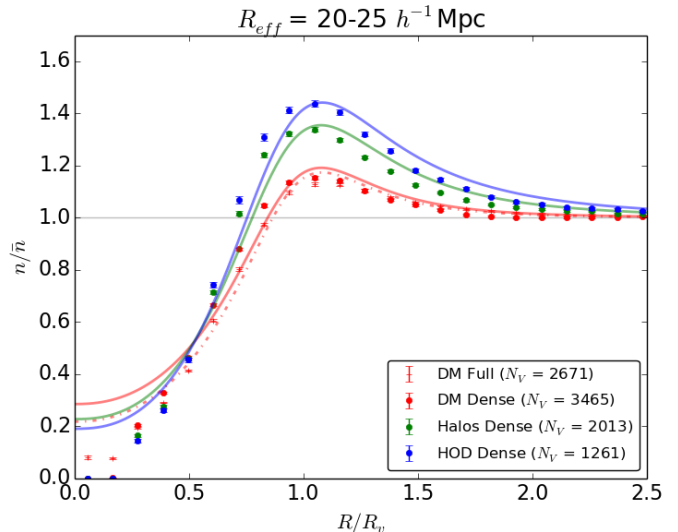


Figure 8: Example one-dimensional radial density profiles of stacked voids (points with error bars) and best-fit curves (thin lines) using the HSW profile. Each profile is normalized to the mean number density  $\bar{n}$  of that sample and  $R_v$  corresponds to the median void size in the stack. *Reproduced from Sutter et al. (2013a).*

## 5. Quick-Start Guide

VIDE uses Python and C++, and so requires only a few prerequisites prior to installation: namely, CMake, Python 2.7, NumPy ( $\geq 1.6.1$ ), and Matplotlib ( $\geq 1.1.rc$ ). VIDE will, by default, automatically download and install all other required Python and C++ libraries (healpy, cython, GSL, Boost, etc.), unless the user indicates via a setup parameter that the libraries are already available on the system.

After installation, the user should move to the `pipeline/datasets` directory and create a `dataset` file. The dataset describes the observation or simulation parameters, listing of input files, the desired subsampling levels, and various other bookkeeping parameters. Inputs are prepared with `prepareInputs`, which organizes and (if necessary) converts inputs, creates void-finding pipeline scripts, and performs subsampling or HOD generation if requested by the user.

The user runs the command `generateCatalog` on each pipeline script. This command performs the actual void finding in three stages: 1) further processing of inputs (e.g., application of boundary particles) for compatibility with ZOBOV, 2) void finding, and 3) filtering of voids near boundaries, construction of the void hierarchy, and generation of void property summary outputs.

After void finding VIDE provides a Python library (`void_python_tools.voidUtil`) for loading, manipulating, and analyzing the resulting void catalogs, as presented in the previous section. The user simply loads a catalog by pointing to an output directory, and has immediate access to all void properties and member galaxies. Using this loaded catalog the user may exploit all the functionality

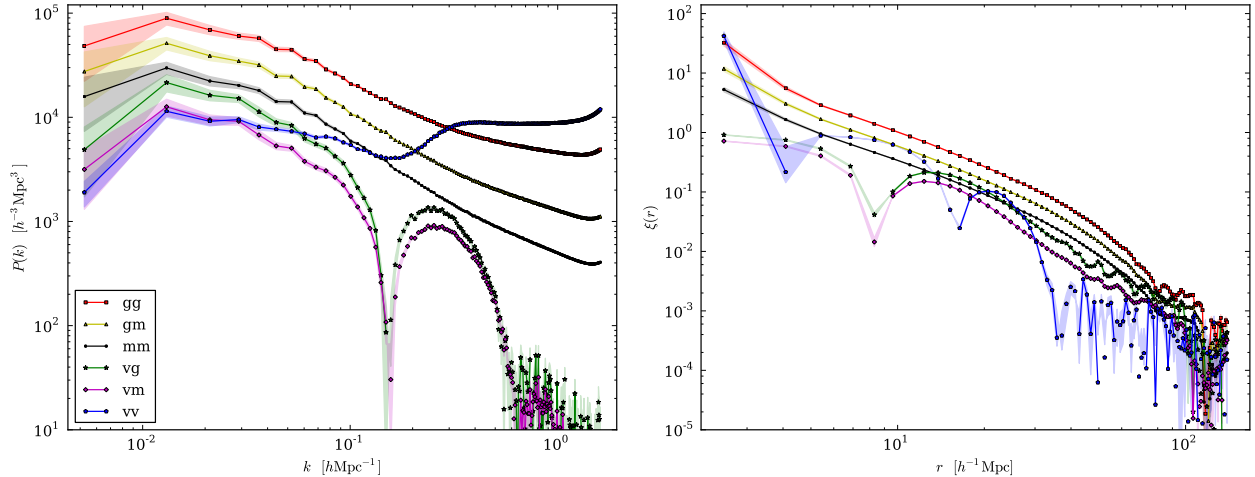


Figure 7: Example power spectra (left) and correlation functions (right) for various combinations of dark matter particles, mock galaxies, and voids (see inset, solid lines omitted for negative values). Shaded bands show  $1\sigma$ -uncertainties estimated from scatter in the bin average. *Reproduced from Hamaus et al. (2014b).*

described above.

Complete documentation is available at [http://bitbucket.org/cosmicvoids/vid\\_e\\_public/wiki/](http://bitbucket.org/cosmicvoids/vid_e_public/wiki/).

## 6. Conclusions

We have presented and discussed the capabilities of VIDE, a new Python/C++ toolkit for identifying cosmic voids in cosmological simulations and galaxy redshift surveys. VIDE performs void identification using a substantially modified and enhanced version of the watershed code ZOBOV. The modifications mostly improve the speed and robustness of the original implementation, as well as adding extensions to handle observational survey geometries within the watershed framework. Furthermore, VIDE is able to support a variety of mock and real datasets, and provides extensive and flexible tools for loading and analyzing void catalogs. We have highlighted these analysis tools (filtering, plotting, clustering statistics, stacking, profile fitting, etc.) using examples from previous and current research using VIDE.

The analysis toolkit enables a wide variety of both theoretical and observational void research. For example, the myriad basic and derived void properties available to the user, such as sky positions, shapes, and sizes, permit simple explorations of void properties and cross-correlation with other datasets. Extracting void member particles and their associated volumes can be used for examining galaxy properties in low-density environments. Cross-matching is useful for understanding the impacts of peculiar velocities or galaxy bias, as well as providing a platform for studying the effects of modified gravity or fifth forces on a void-by-void basis. Void power spectra, shape distributions, number functions, and density profiles, easily accessible via VIDE, are sensitive probes of cosmology. Users may also access previously-fit HSW density profiles, enabling

theoretical predictions of the ISW or gravitational lensing signals. The ease of filtering the void catalog on various criteria allow the user to optimize the selection of voids to maximize the scientific return for their particular research aims.

While the current release version of VIDE is fully functional, we do plan a number of further enhancements, such as integrating the HOD fitting routines directly into the pipeline (rather than the standalone version currently packaged), relaxing the ZOBOV constraint of cubic boxes, and implementing angular selection functions. In the immediate future we will add more plotting functionality and include two-dimensional clustering statistic construction capabilities.

VIDE is community-oriented: the code is currently hosted at <http://www.bitbucket.org>, which supports immediate distribution of updates and bug fixes to the user base, as well as providing a host for a wiki and bug tracker. Suggestions and fixes will be incorporated into the code, with numbered versions serving as milestones. Users may utilize the `git` functionality to create branches, make modifications, and request merging of their changes into the main release. We have designed VIDE to be as modular as possible: while currently based on ZOBOV, any void finder that accepts and outputs similar data formats can be included within the toolkit.

There has been an explosive growth in void interest and research in the past decade, as indicated by the number of published void-finding algorithms, studies of void properties, and investigations of cosmological probes. The release of VIDE is in direct response to the growing demand for simple, fast, scalable, and robust tools for finding voids and exploiting their properties for scientific gain. By designing VIDE to be extensible and modular the platform can easily grow to meet the needs of current and future void communities.

The VIDE code and documentation is currently hosted at [http://bitbucket.org/cosmicvoids/vide\\_public](http://bitbucket.org/cosmicvoids/vide_public), with links to numbered versions at <http://www.cosmicvoids.net>.

## Acknowledgments

The authors are heavily indebted to Mark Neyrinck, who wisely and generously made ZOBOV publicly available. To recognize that contribution, the authors ask that ZOBOV be cited alongside VIDE.

PMS would like to thank Jeremy Tinker for providing the HOD code used in VIDE.

The authors acknowledge support from NSF Grant NSF AST 09-08693 ARRA. BDW acknowledges funding from an ANR Chaire d'Excellence (ANR-10-CEXC-004-01), the UPMC Chaire Internationale in Theoretical Cosmology, and NSF grants AST-0908 902 and AST-0708849. This work made in the ILP LABEX (under reference ANR-10-LABX-63) was supported by French state funds managed by the ANR within the Investissements d'Avenir programme under reference ANR-11-IDEX-0004-02.

## References

- Aragon-Calvo, M.A., Szalay, A.S., 2013. The hierarchical structure and dynamics of voids. *Mon. Not. R. Astron. Soc.* 428, 3409–3424. doi:10.1093/mnras/sts281, arXiv:1203.0248.
- Barber, C.B., Dobkin, D.P., Huhdanpaa, H., 1996. The quickhull algorithm for convex hulls. *ACM Trans. Math. Softw.* 22, 469–483. URL: <http://doi.acm.org/10.1145/235815.235821>, doi:10.1145/235815.235821.
- Beck, A.M., Hanasz, M., Lesch, H., Remus, R.S., Stasyszyn, F.A., 2013. On the magnetic fields in voids. *Mon. Not. R. Astron. Soc.* 429, L60–L64. doi:10.1093/mnrasl/sls026, arXiv:1210.8360.
- Benson, A.J., Hoyle, F., Torres, F., Vogeley, M.S., 2003. Galaxy voids in cold dark matter universes. *Mon. Not. R. Astron. Soc.* 340, 160–174. URL: <http://adsabs.harvard.edu/abs/2003MNRAS.340..160B>, doi:10.1046/j.1365-8711.2003.06281.x.
- Berlind, A.A., Weinberg, D.H., 2002. The Halo Occupation Distribution: Toward an Empirical Determination of the Relation between Galaxies and Mass. *ApJ* 575, 587–616. doi:10.1086/341469, arXiv:arXiv:astro-ph/0109001.
- Biswas, R., Alizadeh, E., Wandelt, B.D., 2010. Voids as a precision probe of dark energy. *Phys. Rev. D* 82, 023002. doi:10.1103/PhysRevD.82.023002, arXiv:1002.0014.
- Bos, E.G.P., van de Weygaert, R., Dolag, K., Pettorino, V., 2012. The darkness that shaped the void: dark energy and cosmic voids. ArXiv e-prints: 1205.4238 arXiv:1205.4238.
- Cai, Y.C., Neyrinck, M.C., Szapudi, I., Cole, S., Frenk, C.S., 2014. A Possible Cold Imprint of Voids on the Microwave Background Radiation. *ApJ* 786, 110. doi:10.1088/0004-637X/786/2/110, arXiv:1301.6136.
- Carlesi, E., Knebe, A., Lewis, G.F., Wales, S., Yepes, G., 2014. Hydrodynamical simulations of coupled and uncoupled quintessence models - I. Halo properties and the cosmic web. *Mon. Not. R. Astron. Soc.* 439, 2943–2957. doi:10.1093/mnras/stu150, arXiv:1401.5005.
- Cautun, M., van de Weygaert, R., Jones, B.J.T., 2013. NEXUS: tracing the cosmic web connection. *Mon. Not. R. Astron. Soc.* 429, 1286–1308. doi:10.1093/mnras/sts416, arXiv:1209.2043.
- Ceccarelli, L., Herrera-Camus, R., Lambas, D.G., Galaz, G., Padilla, N.D., 2012. Low and high surface brightness galaxies at void walls. *Mon. Not. R. Astron. Soc.* 426, L6–L10. doi:10.1111/j.1745-3933.2012.01311.x, arXiv:1207.4203.
- Clampitt, J., Cai, Y.C., Li, B., 2013. Voids in modified gravity: excursion set predictions. *Mon. Not. R. Astron. Soc.* 431, 749–766. doi:10.1093/mnras/stt219, arXiv:1212.2216.
- Clampitt, J., Jain, B., 2014. Lensing Measurements of the Mass Distribution in SDSS Voids. ArXiv e-prints: 1404.1834 arXiv:1404.1834.
- Dubey, A., Reid, L.B., Fisher, R., 2008. Introduction to FLASH 3.0, with application to supersonic turbulence. *Physica Scripta* T132, 014046. URL: <http://adsabs.harvard.edu/abs/2008PhST..132a4046D>, doi:10.1088/0031-8949/2008/T132/014046.
- Dubinski, J., da Costa, L.N., Goldwirth, D.S., Lecar, M., Piran, T., 1993. Void evolution and the large-scale structure. *ApJ* 410, 458. URL: <http://adsabs.harvard.edu/abs/1993ApJ...410..458D>, doi:10.1086/172762.
- Fillmore, J.A., Goldreich, P., 1984. Self-similar spherical voids in an expanding universe. *ApJ* 281, 9. URL: <http://adsabs.harvard.edu/abs/1984ApJ...281...9F>, doi:10.1086/162071.
- Goldberg, D.M., Vogeley, M.S., 2004. Simulating Voids. *ApJ* 605, 1–6. URL: <http://adsabs.harvard.edu/abs/2004ApJ...605...1G>, doi:10.1086/382143.
- Gorski, K.M., Hivon, E., Banday, A.J., Wandelt, B.D., Hansen, F.K., Reinecke, M., Bartelmann, M., 2005. HEALPix: A Framework for HighResolution Discretization and Fast Analysis of Data Distributed on the Sphere. *ApJ* 622, 759. URL: <http://adsabs.harvard.edu/abs/2005ApJ...622..759G>, doi:10.1086/427976.
- Gottlober, S., Lokas, E.L., Klypin, A., Hoffman, Y., 2003. The structure of voids. *Mon. Not. R. Astron. Soc.* 344, 715–724. URL: <http://adsabs.harvard.edu/abs/2003MNRAS.344..715G>, doi:10.1046/j.1365-8711.2003.06850.x.
- Granett, B.R., Neyrinck, M.C., Szapudi, I., 2008. An Imprint of Superstructures on the Microwave Background due to the Integrated Sachs-Wolfe Effect. *ApJ* 683, L99–L102. doi:10.1086/591670, arXiv:0805.3695.
- Gregory, S.A., Thompson, L.A., 1978. The Coma/A1367 supercluster and its environs. *ApJ* 222, 784–799. doi:10.1086/156198.
- Hamaus, N., Sutter, P.M., Wandelt, B.D., 2014a. ArXiv e-prints: 1403.5499.
- Hamaus, N., Wandelt, B.D., Sutter, P.M., Lavaux, G., Warren, M.S., 2014b. Cosmology with Void-Galaxy Correlations. *Physical Review Letters* 112, 041304. doi:10.1103/PhysRevLett.112.041304, arXiv:1307.2571.
- Hockney, R. W. & Eastwood, J. W. (Ed.), 1988. Computer simulation using particles.
- Hoyle, F., Vogeley, M.S., 2004. Voids in the TwoDegree Field Galaxy Redshift Survey. *ApJ* 607, 751–764. URL: <http://adsabs.harvard.edu/abs/2004ApJ...607..751H>, doi:10.1086/386279.
- Hoyle, F., Vogeley, M.S., Pan, D., 2012. Photometric properties of void galaxies in the Sloan Digital Sky Survey Data Release 7. *Mon. Not. R. Astron. Soc.* 426, 3041–3050. doi:10.1111/j.1365-2966.2012.21943.x, arXiv:1205.1843.
- Ilić, S., Langer, M., Douspis, M., 2013. Detecting the integrated Sachs-Wolfe effect with stacked voids. *Astron. & Astrophys.* 556, A51. doi:10.1051/0004-6361/201321150, arXiv:1301.5849.
- Jõeveer, M., Einasto, J., Tago, E., 1978. Spatial distribution of galaxies and of clusters of galaxies in the southern galactic hemisphere. *Mon. Not. R. Astron. Soc.* 185, 357–370.
- Kirshner, R.P., Oemler, A., Schechter, P.L., Shectman, S.A., 1981. A million cubic megaparsec void in Bootes. *ApJ* 248, L57. URL: <http://adsabs.harvard.edu/abs/1981ApJ...248L..57K>, doi:10.1086/183623.
- Kreckel, K., Ryan Joung, M., Cen, R., 2011. SIMULATED VOID GALAXIES IN THE STANDARD COLD DARK MATTER MODEL. *ApJ* 735, 132. URL: <http://adsabs.harvard.edu/abs/2011ApJ...735..132K>, doi:10.1088/0004-637X/735/2/132.
- Lavaux, G., Wandelt, B.D., 2010. Precision cosmology with voids: definition, methods, dynamics. *Mon. Not. R. Astron. Soc.* 403, 1392–1408. doi:10.1111/j.1365-2966.2010.16197.x, arXiv:0906.4101.
- Lavaux, G., Wandelt, B.D., 2012. Precision Cosmography with Stacked Voids. *ApJ* 754, 109. doi:10.1088/0004-637X/754/2/109, arXiv:1110.0345.

- Li, B., Zhao, G.B., Koyama, K., 2012. Haloes and voids in  $f(R)$  gravity. *Mon. Not. R. Astron. Soc.* 421, 3481–3487. doi:10.1111/j.1365-2966.2012.20573.x, arXiv:1111.2602.
- Melchior, P., Sutter, P.M., Sheldon, E.S., Krause, E., Wandelt, B.D., 2014. First measurement of gravitational lensing by cosmic voids in SDSS. *Mon. Not. R. Astron. Soc.* 440, 2922–2927. doi:10.1093/mnras/stu456, arXiv:1309.2045.
- Nadathur, S., Hotchkiss, S., 2014. A robust public catalogue of voids and superclusters in the SDSS Data Release 7 galaxy surveys. *Mon. Not. R. Astron. Soc.* 440, 1248–1262. doi:10.1093/mnras/stu349, arXiv:1310.2791.
- Navarro, J.F., Frenk, C.S., White, S.D.M., 1996. The Structure of Cold Dark Matter Halos. *ApJ* 462, 563. doi:10.1086/177173, arXiv:astro-ph/9508025.
- Neyrinck, M.C., 2008. zobov: a parameter-free void-finding algorithm. *Mon. Not. R. Astron. Soc.* 386, 2101–2109. URL: <http://adsabs.harvard.edu/abs/2008MNRAS.386.2101N>, doi:10.1111/j.1365-2966.2008.13180.x.
- Neyrinck, M.C., Aragón-Calvo, M.A., Jeong, D., Wang, X., 2014. A halo bias function measured deeply into voids without stochasticity. *Mon. Not. R. Astron. Soc.* 441, 646–655. doi:10.1093/mnras/stu589, arXiv:1309.6641.
- Neyrinck, M.C., Falck, B.L., Szalay, A.S., 2013. ORIGAMI: Delineating Cosmic Structures with Phase-Space Folds. ArXiv e-prints: 1309.4787 arXiv:1309.4787.
- Neyrinck, M.C., Gnedin, N.Y., Hamilton, A.J.S., 2005. VOBOS: an almost-parameter-free halo-finding algorithm. *Mon. Not. R. Astron. Soc.* 356, 1222–1232. doi:10.1111/j.1365-2966.2004.08505.x, arXiv:astro-ph/0402346.
- Padilla, N.D., Ceccarelli, L., Lambas, D.G., 2005. *Mon. Not. R. Astron. Soc.* 363, 977–990.
- Pan, D.C., Vogeley, M.S., Hoyle, F., Choi, Y.Y., Park, C., 2012. Cosmic voids in Sloan Digital Sky Survey Data Release 7. *Mon. Not. R. Astron. Soc.* 421, 926–934. doi:10.1111/j.1365-2966.2011.20197.x, arXiv:1103.4156.
- Pisani, A., Lavaux, G., Sutter, P.M., Wandelt, B.D., 2013. Real-space density profile reconstruction of stacked voids. ArXiv e-prints: 1306.3052 arXiv:1306.3052.
- Pisani, A., Sutter, P.M., Wandelt, B.D., 2014. in prep.
- Planck Collaboration, 2013. Planck 2013 results. XIX. The integrated Sachs-Wolfe effect. ArXiv e-prints: 1303.5079 arXiv:1303.5079.
- Platen, E., van de Weygaert, R., Jones, B.J.T., 2007. A cosmic watershed: the WVF void detection technique. *Mon. Not. R. Astron. Soc.* 380, 551–570. URL: <http://adsabs.harvard.edu/abs/2007MNRAS.380..551P>, doi:10.1111/j.1365-2966.2007.12125.x.
- Ricciardelli, E., Quilis, V., Varela, J., 2014. On the universality of void density profiles. *Mon. Not. R. Astron. Soc.* 440, 601–609. doi:10.1093/mnras/stu307, arXiv:1402.2976.
- Rieder, S., van de Weygaert, R., Cautun, M., Beygu, B., Portegies Zwart, S., 2013. Assembly of filamentary void galaxy configurations. *Mon. Not. R. Astron. Soc.* 435, 222–241. doi:10.1093/mnras/stt1288, arXiv:1307.7182.
- Sousbie, T., 2011. The persistent cosmic web and its filamentary structure - I. Theory and implementation. *Mon. Not. R. Astron. Soc.* 414, 350–383. doi:10.1111/j.1365-2966.2011.18394.x, arXiv:1009.4015.
- Spolyar, D., Sahlén, M., Silk, J., 2013. Topology and Dark Energy: Testing Gravity in Voids. ArXiv e-prints arXiv:1304.5239.
- Springel, V., 2005. The cosmological simulation code GADGET-2. *Mon. Not. R. Astron. Soc.* 364, 1105–1134. doi:10.1111/j.1365-2966.2005.09655.x, arXiv:astro-ph/0505010.
- Sutter, P.M., Carlesi, E., Wandelt, B.D., Knebe, A., 2014a. in prep.
- Sutter, P.M., Elahi, P., Falck, B., Onions, J., Hamaus, N., Knebe, A., Srisawat, C., Schneider, A., 2014b. The life and death of cosmic voids. ArXiv e-prints: 1403.7525 arXiv:1403.7525.
- Sutter, P.M., Lavaux, G., Wandelt, B.D., Hamaus, N., Weinberg, D.H., Warren, M.S., 2013a. Sparse sampling, galaxy bias, and voids. ArXiv e-prints arXiv:1309.5087.
- Sutter, P.M., Lavaux, G., Wandelt, B.D., Weinberg, D.H., 2012a. A First Application of the Alcock-Paczynski Test to Stacked Cosmic Voids. *ApJ* 761, 187. doi:10.1088/0004-637X/761/2/187, arXiv:1208.1058.
- Sutter, P.M., Lavaux, G., Wandelt, B.D., Weinberg, D.H., 2012b. A Public Void Catalog from the SDSS DR7 Galaxy Redshift Surveys Based on the Watershed Transform. *ApJ* 761, 44. doi:10.1088/0004-637X/761/1/44, arXiv:1207.2524.
- Sutter, P.M., Lavaux, G., Wandelt, B.D., Weinberg, D.H., 2013b. A response to arXiv:1310.2791: A self-consistent public catalogue of voids and superclusters in the SDSS Data Release 7 galaxy surveys. ArXiv e-prints: 1310.5067 arXiv:1310.5067.
- Sutter, P.M., Lavaux, G., Wandelt, B.D., Weinberg, D.H., Warren, M.S., 2013c. Voids in the SDSS DR9: observations, simulations, and the impact of the survey mask. ArXiv e-prints: 1310.7155 arXiv:1310.7155.
- Sutter, P.M., Lavaux, G., Wandelt, B.D., Weinberg, D.H., Warren, M.S., 2014c. The dark matter of galaxy voids. *Mon. Not. R. Astron. Soc.* 438, 3177–3187. doi:10.1093/mnras/stt2425, arXiv:1311.3301.
- Sutter, P.M., Pisani, A., Wandelt, B.D., 2014d. A measurement of the Alcock-Paczynski test using cosmic voids in the SDSS. ArXiv e-prints: 1404.5618 arXiv:1404.5618.
- Taylor, A.M., Vovk, I., Neronov, A., 2011. Extragalactic magnetic fields constraints from simultaneous GeV-TeV observations of blazars. *Astron. & Astrophys.* 529, A144. doi:10.1051/0004-6361/201116441, arXiv:1101.0932.
- Tejos, N., Morris, S.L., Crighton, N.H.M., Theuns, T., Altay, G., Finn, C.W., 2012. Large-scale structure in absorption: gas within and around galaxy voids. *Mon. Not. R. Astron. Soc.* 425, 245–260. doi:10.1111/j.1365-2966.2012.21448.x, arXiv:1205.2697.
- Teyssier, R., 2002. Cosmological hydrodynamics with adaptive mesh refinement. A new high resolution code called RAMSES. *Astron. & Astrophys.* 385, 337–364. doi:10.1051/0004-6361:20011817, arXiv:astro-ph/0111367.
- Thompson, K.L., Vishniac, E.T., 1987. The effect of spherical voids on the microwave background radiation. *ApJ* 313, 517. URL: <http://adsabs.harvard.edu/abs/1987ApJ...313..517T>, doi:10.1086/164991.
- van de Weygaert, R., Platen, E., 2011. Cosmic Voids: Structure, Dynamics and Galaxies. *International Journal of Modern Physics Conference Series* 1, 41–66. doi:10.1142/S2010194511000092, arXiv:0912.2997.
- van de Weygaert, R., van Kampen, E., 1993. Voids in Gravitational Instability Scenarios - Part One - Global Density and Velocity Fields in an Einstein - De-Sitter Universe. *Mon. Not. R. Astron. Soc.* 263, 481.
- van de Weygaert, R., Vegter, G., Platen, E., Eldering, B., Kruithof, N., 2010a. Alpha Shape Topology of the Cosmic Web. ArXiv e-prints arXiv:1006.2765.
- van de Weygaert, R., et al., 2010b. The Cosmically Depressed: Life, Sociology and Identity of Voids, in: Verdes-Montenegro, L., Del Olmo, A., Sulentic, J. (Eds.), *Galaxies in Isolation: Exploring Nature Versus Nurture*, p. 99. arXiv:0912.3473.
- Warren, M.S., 2013. 2HOT: An Improved Parallel Hashed Oct-Tree N-Body Algorithm for Cosmological Simulation, in: *Proceedings of SC13: International Conference for High Performance Computing, Networking, Storage and Analysis*, ACM. p. 72. arXiv:1310.4502.
- Zheng, Z., Coil, A.L., Zehavi, I., 2007. Galaxy Evolution from Halo Occupation Distribution Modeling of DEEP2 and SDSS Galaxy Clustering. *ApJ* 667, 760–779. doi:10.1086/521074, arXiv:arXiv:astro-ph/0703457.